Effect of Boron Segregation at Grain Boundaries on Heat-Affected Zone Cracking in Wrought INCONEL 718

W. CHEN, M.C. CHATURVEDI, and N.L. RICHARDS

Susceptibility to heat-affected zone (HAZ) cracking during electron-beam welding was studied in two INCONEL 718–based alloys doped with different levels of boron. By lowering the carbon, sulfur, and phosphorous concentrations to be "as low as possible," the occurrence of HAZ cracking was related directly to the level of segregation of boron at grain boundaries, which occurred by nonequilibrium segregation during a preweld heat treatment. The study has demonstrated a direct correlation between the amount of boron segregated at grain boundaries and their susceptibility to HAZ cracking, in terms of the total crack length and number of cracks observed in the HAZ. The analysis of results suggests that both the melting and resolidification temperatures of the boron-segregated grain boundaries can be about 100 °C to 200 °C lower than those of the grain boundaries that were susceptible to constitutional liquation of Nb carbides on them, making boron more deleterious in causing HAZ cracking.

I. INTRODUCTION

HEAT-AFFECTED zone (HAZ) liquation cracking in INCONEL 718* has been extensively studied and has been attributed to different factors. The original theory of liquation cracking was related to the formation of grain-boundary liquid through the constitutional liquation of grain-boundary precipitates and the inability of the liquid films to support the tensile stress developed during cooling after welding.[1,2,3] The phases that may induce constitutional liquation in the alloy have been identified to be primarily NbC carbides[1,2,4–6] in wrought material and carbides and Laves phase[5,7,8] in the cast alloy.

*INCONEL is a trademark of INCO Alloys, Huntington, WV.

The application of the constitutional liquation mechanism to HAZ cracking is generally satisfactory, yet is challenged by some observations. For example, the alloy's resistance or susceptibility to HAZ liquation cracking is not proportional to the volume fraction of grain-boundary precipitates that are prone to constitutional liquation, but is significantly influenced by heat treatment, which, in fact, may not cause a significant change in the grain-boundary precipitation phases likely to undergo constitutional liquation.[5] When material was found not to contain grain-boundary precipitates, a susceptibility to HAZ liquation cracking still existed. Borland,[9] for example, in 1960, suggested that segregation of elements with high relative potency factor values (leading to wide freezing ranges), combined with suitable wetting of grain surfaces, could result in weld cracking. Other possibilities, according to Savage and Krantz,[10] include sweeping up of solute by migrating boundaries and the influx of solute down the grain boundaries due to epitaxial effects from the weld pool. Thus, several possibilities exist to enable species to segregate on grain boundaries and reduce the melting temperature of the grain boundaries relative to the surrounding matrix.

The segregation of impurities to grain boundaries can take place during the heat treatment before welding. In general, it can occur by two mechanisms, *viz.*, equilibrium segregation[11] and nonequilibrium segregation.[12–19] In equilibrium segregation, solute atoms that diffuse to grain boundaries are actually bound to grain-boundary sites. The extent of this segregation increases with decreasing temperature and increasing solute concentration in the matrix. Nonequilibrium segregation occurs during cooling from high temperature[13,15,16] and during annealing following plastic deformation.[20,21] This type of segregation requires the formation of solute-vacancy complexes and a concentration gradient of these complexes between the grain interiors and grain boundaries. The annihilation of vacancies at grain boundaries causes a concentration gradient of complexes, which drives the complexes to diffuse from within the grain to the grain boundaries. This diffusion causes excessive solute atoms to concentrate in the vicinity of grain boundaries. The degree of nonequilibrium segregation has been found to depend on the starting temperature, cooling rate, and bulk concentration of solutes.[12–19]

The segregation of impurities can also take place during the welding process.[22,23] The occurrence of equilibrium segregation in this case might be dependent on the temperature to which the material is exposed and the diffusion time that is available. If heating and cooling rates are rapid, it may not be possible for the impurities to travel to the grain boundaries, which is a function of the diffusivity of the impurities and the time available for their diffusion. The nonequilibrium segregation takes place during the cooling cycle of welding. It, however, may not cause HAZ cracking if the temperature in the HAZ has been reduced to the level at which the melting of segregated grain boundaries is unlikely. A grain-boundary sweeping mechanism has been also proposed to account for the segregation during welding.[10,22,23] It is suggested that, as grain boundaries migrate upon heating above the threshold grain-growth temperature,

W. CHEN, Assistant Professor, is with the Department of Chemical and Materials Engineering, University of Alberta, Edmonton, AB, Canada T6G 2G6. M.C. CHATURVEDI, Senior NSERC Industrial Research Professor, and N.L. RICHARDS, Associate Professor, are with the Department of Mechanical and Industrial Engineering, University of Manitoba, Winnipeg, MB, Canada R3T 5V6.

Manuscript submitted June 5, 2000.

solute and/or impurity atoms are swept into the boundaries and are dragged along as grain growth proceeds. As the temperature in the HAZ increases above the local grain-boundary melting temperature, liquation occurs and the region of the HAZ within a critical embrittlement temperature range becomes susceptible to liquation cracking. It has been, however, questioned whether the solutes are swept into grain boundaries or the migrated grain boundaries can actually escape the segregated solutes during their migration.[24]

Thompson and co-workers, by Auger spectroscopic analysis of grain-boundary material, have attributed HAZ liquation cracking to the segregation of S on grain boundaries during the preweld heat treatments.[4,25,26] In cast INCONEL 718, Huang *et al.*[27,28] have attributed HAZ liquation cracking to the equilibrium and nonequilibrium segregation of B, the B having been detected by Secondary Ion Mass Spectrometry (SIMS) analysis. The detrimental effect of B was further confirmed by studies on specially prepared INCONEL 718 alloys that had a controlled concentration of B, but were essentially free of S, P, and C.[29] Chaturvedi *et al.*[29] compared the effect of S and B segregation on HAZ liquation cracking of INCONEL 718–based alloys and found that B has much more detrimental effect than S, which supports the earlier suggestion of Kelly.[30]

The SIMS studies of the segregation of B during preweld heat treatment of both cast and wrought INCONEL 718 alloys and the corresponding orientation imaging and electron backscattered diffraction analysis have reasonably well explained the mechanism of the segregation of B and its effect on HAZ liquation cracking.[27,28,29] However, detailed studies on the degree of segregation related to the preweld heat treatment and process and its influence on grain-boundary liquation are lacking. Therefore, experiments were carefully designed to further study the relationship between the grain-boundary segregation of B and the susceptibility to HAZ cracking in wrought INCONEL 718 alloys. Two INCONEL 718–based alloys with identical chemical compositions except for the boron concentration were designed. By controlling the concentration of carbon and phosporus to a level as low as possible, the HAZ cracking due to constitutional liquation was avoided. Various levels of segregation of boron at grain boundaries were obtained through preweld heat treatments according to the grain-boundary segregation behavior of boron in INCONEL 718, as reported elsewhere.[31] The cracking susceptibility of various materials was then related to the degree of segregation.

II. EXPERIMENTAL METHODS

Two INCONEL 718–based alloys were used in this study. Their chemical compositions, as listed in Table I, were identical except for the concentration of boron, which was 43 and 11 ppm, respectively, for the high-boron and low-boron alloys. The carbon, sulphur, and phosphorous in both the alloys were at a level as low as possible, to minimize their influence on HAZ liquation cracking. Cast ingots of these alloys were prepared by Special Metals Corporation (New Hartford, NY) using standard commercial vacuum induction melting (VIM) practice and hot rolled to 12.5-mm-thick plates. Sections of the alloys, measuring 12.5 × 12.5 mm, were solution treated at 1200 °C for 2 hours to produce precipitate-free microstructures and then water quenched.

Table I. Chemical Compositions (Weight Percent) of INCONEL 718

Elements*	Low Boron Material	High Boron Material
C	0.003	0.002
Si	0.02	0.02
Cr	18.85	18.84
Ni	52.36	52.43
Fe	19.12	19.02
Mo	3.01	3.01
Nb	5.06	5.09
Ti	0.99	1.00
Al	0.49	0.49
B	0.0011	0.0043
S	0.0008	0.0009
P	0.006	0.007
W	0.02	0.02

*About 0.01 wt pct of Mn, Hf, Ta, Cu, V, and Co was also detected in both alloys.

The solution-treated specimens were given a succession of deformation and annealing treatments at 1030 °C to produce a single-phase microstructure with a grain size of about 100 μm for both the materials. Two 30-mm-long specimens of both the alloys were given a final solution treatment at 1050 °C, 1100 °C, and 1150 °C for 9.6, 7.2, and 5.5. minutes, respectively. The different heat-treatment times used in the final heat treatment were determined according to d^2/D[32] where $D = 2 \times 10^{-7} \exp(-0.91\ ev/kT)m^2/s$[31] is the diffusion coefficient of *B*, and *d* is the diffusion distance of boron, which was set to be equal to 4 times the grain size in order to achieve the same level of equilibrium segregation of boron at grain boundaries. After the solution treatment at each of these temperatures, one set of specimens was air cooled and the other one was water quenched. The cooling rates were measured to be 570 °C/s during water quenching and 117 °C/s during the initial stages of air cooling.[31] After the final heat treatment, the specimens were electron-beam welded by the bead-on-plate technique by a Mark VII EB Welder, using a sharp focus (without beam oscillation) at 44 kV, 79 mA, and 152 cm/min. This welding procedure produced partial-penetration welds. Cross sections of the welded specimens were mounted and polished and given a light etch for the microstructural examination. The HAZ crack measurements were done on an analytical JEOL* 840 scanning electron microscope equipped with a Noran stored-image analysis program.

*JEOL is a trademark of Japan Electron Optics Ltd., Tokyo.

III. RESULTS AND DISCUSSION

A. *Microstructural Observations*

The microstructure of the as-received hot-rolled material consisted of austenitic grains with large amount of Laves phase. A very small amount of carbides was also observed. To produce a single-phase material, the alloys were first heated to 1000 °C and then to 1200 °C for 1 hour at a very slow rate of 70 °C/h to prevent the liquation of Laves phase. The solution-treated and water-quenched material was essentially single phase, but with a very large grain size. Therefore,

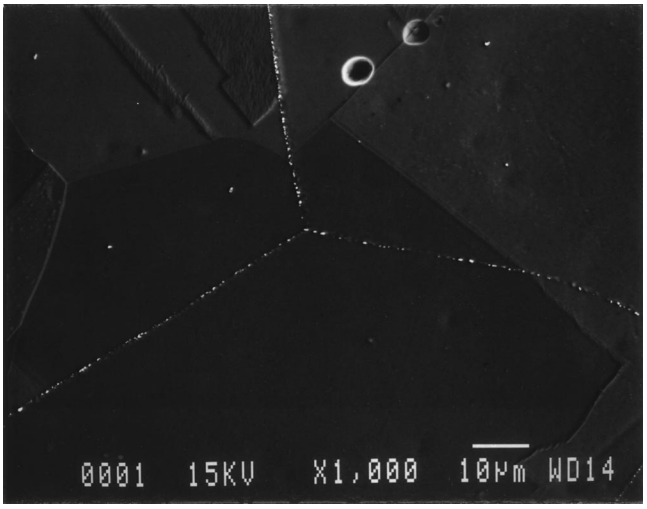

(*a*)

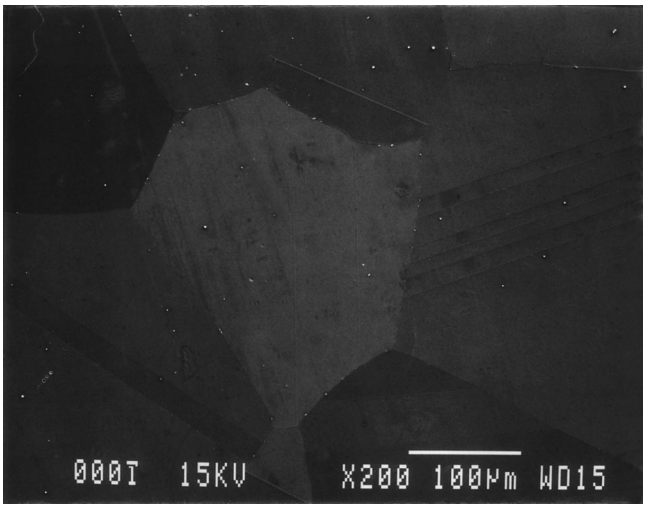

(*b*)

Fig. 1—Microstructures of high boron alloy subjected to solution heat treatment at 1200 °C for 2 h and followed by 25 pct cold rolling and subsequent annealing at 1030 °C for (*a*) 7 h and (*b*) 24 h, respectively.

the material was 25 pct deformed by cold rolling and annealed at 1030 °C, which is the lowest temperature at which a single-phase material can be produced, as it is above the solvus temperature of the Laves phase and δ phase.[33] Moreover, as was reported elsewhere,[31] annealing at 1030 °C first produced borides at the original γ grain boundaries (Figure 1(a)), and the material had to be annealed for 24 hours to dissolve them (Figure 1(b)). It is suggested that new grains nucleated at the original boundaries in the deformed material and consumed the deformed material on both sides of the original boundary to create a new defect-free crystal. This phenomenon was not observed in the low-boron material because of the smaller degree of boron segregation at the grain boundary.[31] On extended annealing, the borides in both the alloys dissolved, but the grain size enlarged to about 200 μm. Therefore, the alloys were given another 25 pct cold deformation, followed by the second annealing at 1030 °C for 4 hours and were then water quenched. The microstructure of the two alloys after the treatment was essentially single phase, with a grain size of about 100 μm.

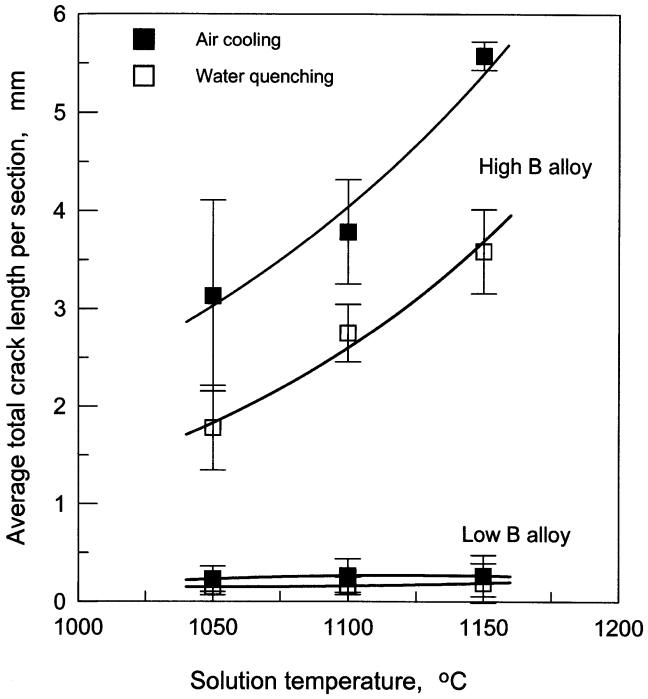

Fig. 2—Effect of solution temperature and cooling rate on the average total crack length per weldment section in HAZ.

After a succession of deformation and annealing treatments at 1030 °C, as described in the previous paragraph, two specimens of each of the two alloys were given a final solution treatment at 1050 °C, 1100 °C, and 1150 °C for 9.6, 7.2, and 5.5 minutes, respectively. These different holding times were used to ensure the same level of equilibrium segregation of boron at grain boundaries in specimens annealed at different temperatures. This short annealing time did not change the grain size of the material. As was reported earlier, these treatments produced different levels of non-equilibrium segregation of B on grain boundaries.[31]

B. *Susceptibility to HAZ Cracking*

The test pieces, after the final heat treatment, were electron beam–welded using the same parameters. The welded pieces were cut in a direction perpendicular to the welding direction. Eight sections in total were examined for each welded piece. Cracks were all observed in the HAZ, and no cracks in the fusion zone were found. The average value of the total crack length per section for all the welded pieces ($\overline{L}_t$) is plotted against the heat-treatment temperature in Figure 2. It is seen that the value of $\overline{L}_t$ in the high-boron material is in the range of 7 to 20 times larger than that observed in the low-boron material. The value of $\overline{L}_t$ is also a function of cooling rate. In general, the material with air cooling shows a value of $\overline{L}_t$ almost 1.5 times larger than the water-quenched material. The value of $\overline{L}_t$ also decreased significantly as the treatment temperature decreased, especially in high-boron materials.

The average number of cracks per welded section ($\overline{N}_t$) and the average length of a crack ($\overline{L}_i$) for both the materials, as a function of the final heat-treatment temperature, are shown in Figures 3 and 4, respectively. It is seen that the values of $\overline{N}_t$ and $\overline{L}_i$ in the high-boron material are significantly larger than those observed in the low-boron material.

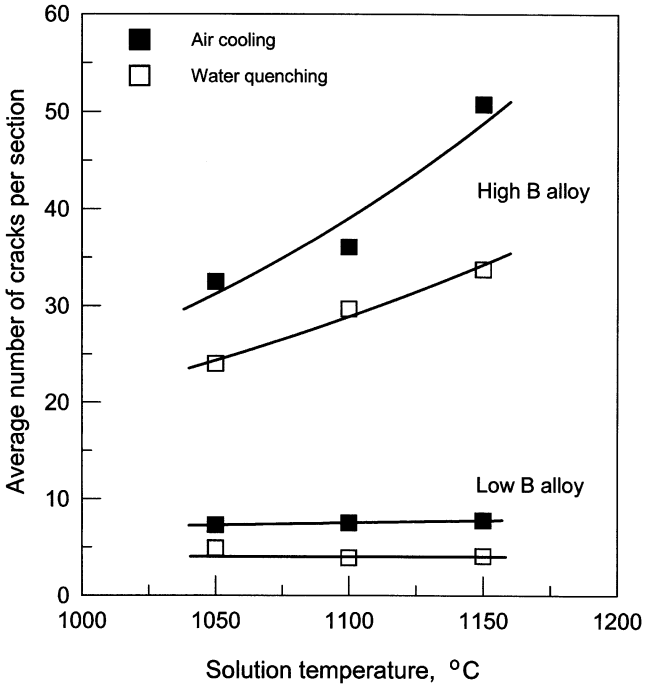

Fig. 3—Effect of solution temperature and cooling rate on the average number of cracks per weldment section in HAZ.

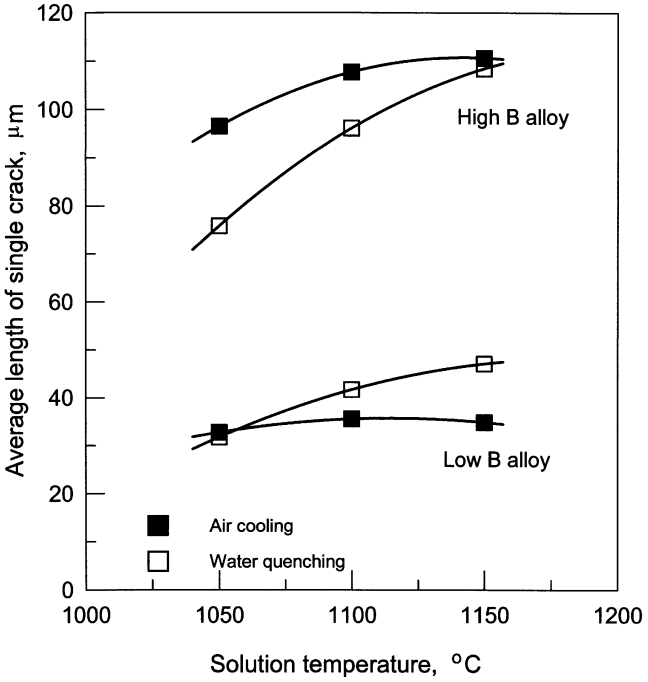

Fig. 4—Effect of solution temperature and cooling rate on the average length of single crack in HAZ.

These two values also decrease with decreasing temperature, but with increasing cooling rate (from air cooling to water quenching), particularly in the high-boron alloy.

The total crack length per section obtained after various heat treatments is related to the number of microcracks per section and to the average length of a single crack, respectively, in Figures 5 and 6. The average length of single crack approaches a limit of about 115 μm. This limit might be a

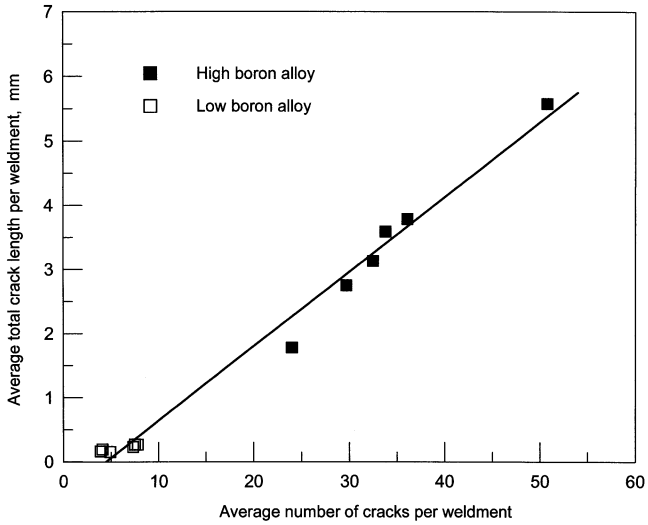

Fig. 5—Relation between the average total crack length per weldment section and the average number of cracks per weldment section.

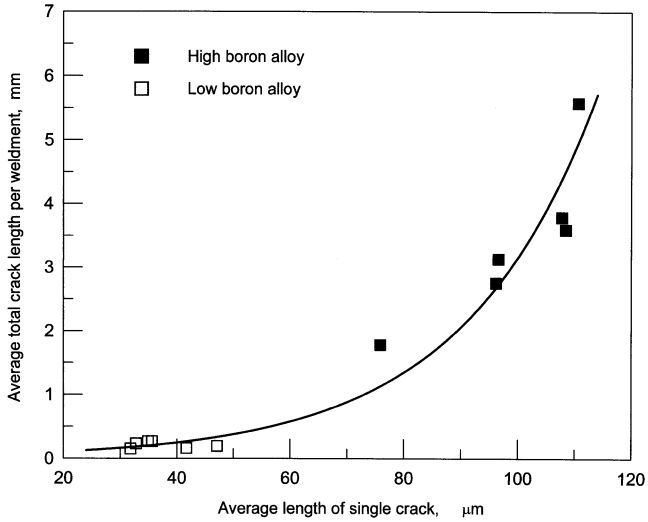

Fig. 6—Change of average total crack length per weldment section with average length of single crack in HAZ.

combined effect of the size of the HAZ and the size of the grains in the HAZ. In the high-boron alloy, the increase in total crack length per section is caused by both the increase in the number of cracks and the length of each crack. In contrast, for the low-boron alloy, the increase in total crack length is more relevant to the increase in the average length of each crack.

C. *Susceptibility to HAZ Cracking* vs *B Grain-Boundary Segregation*

It has been shown previously[27–29,31] that segregation of boron to grain boundaries in these two materials is mainly due to equilibrium and nonequilibrium types, *viz.*, the amount of segregation is a function of the solution-treatment temperature, cooling rate, and solute concentration in the grain matrix. The higher the initial heat-treatment temperature, the larger the concentration of the equilibrium vacancies; therefore, a large number of solute (boron)–vacancy

complexes are available for grain-boundary segregation. Similarly, a small bulk boron concentration produces a small number of solute-vacancy complexes. The nonequilibrium segregation takes place during cooling due to the tendency of vacancy annihilation at grain boundaries. A very fast cooling allows only a limited time for solute-vacancy complexes to diffuse to grain boundaries, while very slow cooling may cause diffusion of already-segregated solutes to the grain interior, due to the solute concentration gradient. Cooling from a higher temperature also permits a longer segregation time and a faster segregation rate than cooling from a lower temperature. This behavior has been demonstrated in an earlier communication[31] and has been reported by other investigators also.[12–19]

To further define the effect of boron on the susceptibility of HAZ liquation cracking, the concentration of boron at grain boundaries arising from the preweld heat treatment was calculated.

Consider a sample that is cooled so rapidly from the solution-treatment temperature (T_0) to an isothermal temperature (T_i) that no mass transfer occurs in the specimen during cooling. Following that, the temperature is maintained at T_i for a period of time. It is suggested that segregation takes place from the very beginning until a critical time is reached, after which desegregation of B due to the increased concentration of B at the grain boundaries will be dominant. The critical time at T_i is given by[14]

$$t_c(T_i) = \frac{d^2 \ln (D_c/D_i)}{4\delta(D_c - D_i)} \qquad [1]$$

Where D_c is the diffusion coefficient of the solute complex in the matrix, D_i is the solute atom diffusion coefficient in the matrix, d is the grain size, and δ is the critical time constant.

To determine the concentration of boron at grain boundaries, the actual segregation time during cooling to room temperature needs to be estimated. This was done by using the effective time concept of continuous cooling.[14,15,16] In this process, a continuous cooling curve was replaced by a corresponding stepped curve, each step of which was formed by a small time and temperature segment so as to closely represent a continuous cooling curve, and the effective time at each temperature step was calculated. The effective time ($t_e(T_i)$) for the stepped curve of n steps at the temperature T_i is given by[14,15,16]

$$t_e(T_i) = \sum_{i=1}^{n} t_i \exp\left(-E_A(T - T_i)/\mathrm{k}TT_i\right) \qquad [2]$$

Where E_A is the activation energy for diffusion of solute atom (boron)–vacancy complexes in the matrix. It is assumed that E_A is given by the average of the values of the vacancy-movement energy and the activation energy for the diffusion of solute atoms.

The functional relation of temperature and cooling time was determined previously to be $T_N = T_0 \exp(-0.4807n\,\Delta t)$ for water quenching and $T_N = T_0 \exp(-0.0977n\,\Delta t)$ for air cooling, respectively.[31]

The other data used for the calculation and the calculated values of t_c and t_e for nonequilibrium segregation of B, for the alloys used in the study, are given in Table II. The critical time to reach the maximum nonequilibrium segregation was calculated to be much longer than the effective segregation time during air cooling and water quenching from 1150 °C, indicating that nonequilibrium segregation was dominant during cooling from the solution-treatment temperature.

Table II. Calculated Values of Nonequilibrium Segregation Time of Boron at Grain Boundaries in INCONEL 718 (Data from Reference 31)

Data Used for Calculation	Calculated Value
$D_c = 1.0 \times 10^{-5} \exp(-0.94\ \mathrm{eV/k}T)$	$t_c(1423\ \mathrm{K}) = 4.82$ s
$D_i = 2.0 \times 10^{-7} \exp(-0.91\ \mathrm{eV/k}T)$	$t_c(900\ \mathrm{K}) = 399$ s
$E_A = 0.94$ eV	
$E_f = 1.4$ eV	$t_e(\mathrm{WQ} - 1423\ \mathrm{K}) = 0.2822$ s
$E_b = -0.94$ eV	$t_e(\mathrm{WQ} - 1373\ \mathrm{K}) = 0.2742$ s
$w = 1.5\ \mu$m	$t_e(\mathrm{WQ} - 1323\ \mathrm{K}) = 0.2657$ s
$d = 100\ \mu$m	$t_e(\mathrm{AC} - 1423\ \mathrm{K}) = 1.473$ s
$\delta = 0.418$	$t_e(\mathrm{AC} - 1373\ \mathrm{K}) = 1.431$ s
$T_i = 900$ K	$t_e(\mathrm{AC} - 1323\ \mathrm{K}) = 1.384$ s

The concentration of B segregated at grain boundaries during a holding time of t ($<t_c$) can be calculated by the following expression.[34]

$$C_b(t) = C_b^m(T_i) - C_g(\alpha_i - \alpha_0) \exp(2\sqrt{D_c t}/\alpha_i w)^2 \operatorname{erfo}(2\sqrt{D_c t}/\alpha_i w) \qquad [3]$$

where $C_b^m(T_i) = C_g(E_b/E_f) \exp((E_b - E_f)/\mathrm{k}T_0 - (E_b - E_f)/\mathrm{k}T_i))$.

In Eq. [3], $C_b^m(T_i)$ is the maximum concentration of nonequilibrium segregation induced during holding at the temperature T_i, α_i and α_0 are the ratios between $C_b^m(T_i)$ and the concentration of solutes within the grain for the isothermal temperature and solution temperature, respectively; t is the isothermal holding time for segregation; w is the width of the segregated layer of solute atoms; E_b and E_f are the energy of formation of the recombined complex and the energy of formation of the vacancy, respectively; and k is the Boltzman's constant.

Equation [3] is used to calculate the segregation at an isothermal condition. However, it is applicable to the segregation during cooling if t_e is used to replace t.[34] The calculated concentration of boron at grain boundaries is given in Table III, which is also plotted in Figures 7 and 8 as a function of $\overline{L}_t$ and $\overline{N}_t$, respectively. Both the figures show a linear relationship between the concentration of boron at grain boundaries and the susceptibility to HAZ liquation cracking in both the alloys. The average length of a crack is seen to increase at a lower boron concentration at grain boundaries, but appears less sensitive to the concentration of boron at grain boundaries as the boron concentration at grain boundaries increases (Figure 9). This is consistent with Figure 6, both of which are due to the fact that a further increase in crack length is limited by the size of the HAZ and, possibly, the grain size as well. This also suggests that the increase in $\overline{L}_t$ with the calculated concentration of B at grain boundaries is primarily caused by the increased number of grain boundaries susceptible to HAZ cracking when more boron is segregated at grain boundaries. However, it is influenced by the increased length of a single crack in the HAZ when less boron is segregated at grain boundaries.

Table III. Calculated Values of Nonequilibrium Segregation Concentration of Boron at Grain Boundaries in INCONEL 718

Alloy	Solution Temperature (°C)	Cooling Rate (°C/s)	$C_b(t)$ (ppm)
High B alloy (C_g = 43 ppm)	1150	570	226.0
	1100	570	213.1
	1050	570	197.3
	1150	117	412.6
	1100	117	372.4
	1050	117	326.9
Low B alloy (C_g = 11 ppm)	1150	570	57.8
	1100	570	54.5
	1050	570	50.5
	1150	117	105.5
	1100	117	95.3
	1050	117	83.6

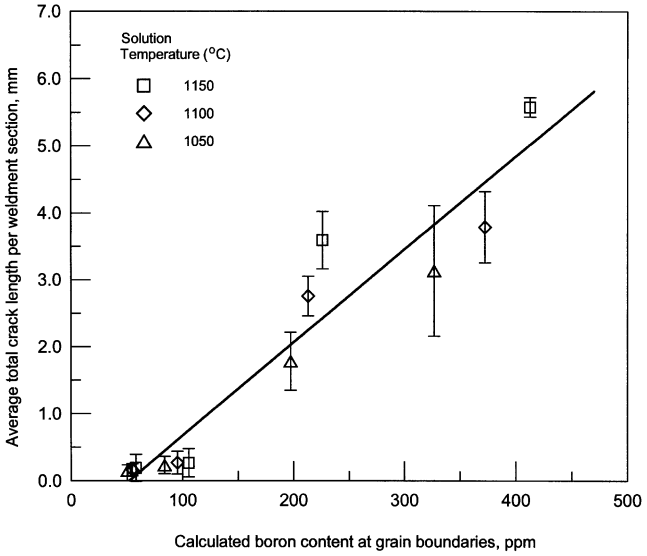

Fig. 7—Dependence of average crack length per weldment section on the calculated boron concentration at grain boundaries.

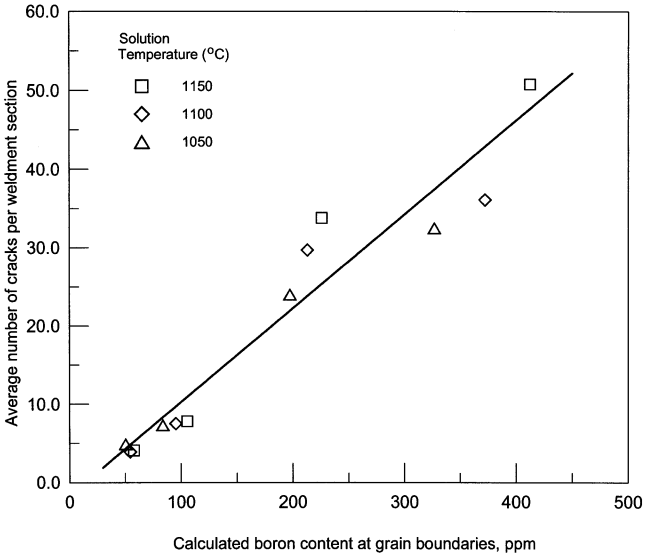

Fig. 8—Dependence of average number of cracks per weldment section on the calculated boron concentration at grain boundaries.

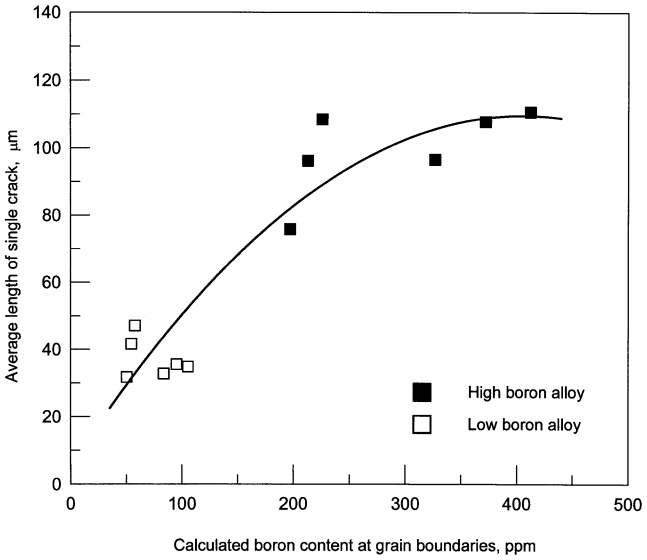

Fig. 9—Variation of average length of single crack with the calculated boron content at grain boundaries.

D. *Formulation of HAZ Cracks at B-Segregated Grain Boundaries*

In general, electron-beam welding produces a nail-shaped fusion zone, and liquation cracks often form in the region around the shoulder of the nail. Figure 10 shows a comparison of microcracks in the nail-shoulder regions in both the two materials. Many more microcracks are seen in the high-boron material than in the low-boron material, and they were observed to have occurred at grain boundaries in the HAZ. The grain size of both the materials was controlled to be identical (about 100 μm), although it may appear to have some variations at some areas. In Figure 10(a), backfilling of cracks near the fusion zone was occasionally observed, which should have an insignificant influence on the crack measurements presented previously.

The segregation of B at grain boundaries decreases the melting point of grain-boundary material and increases the wettability of the grain-boundary surface.[31,35] The melting of grain boundaries near the fusion zone occurred in both the B-doped materials; however, more grain boundaries were melted in the high-boron material than in the low-boron material. Melting of grain boundaries in the HAZ was quite selective, *i.e.*, some grain boundaries were not melted, although they were quite close to the fusion zone. This difference has been attributed to the difference in the level of segregation of B at grain boundaries of different characters, with more segregation occurring at the high-angle boundaries and less at the low-angle and sigma boundaries.[36]

Thompson *et al.*[37] have provided a sequence of events in HAZ liquation cracking of INCONEL 718 material containing Nb carbides or Laves phases. During the heating cycle of welding, Nb carbides or Laves phases start to feed Nb to the matrix through high-temperature diffusion. This, in turn, causes γ + Laves $\rightarrow L$ eutectic melting when the

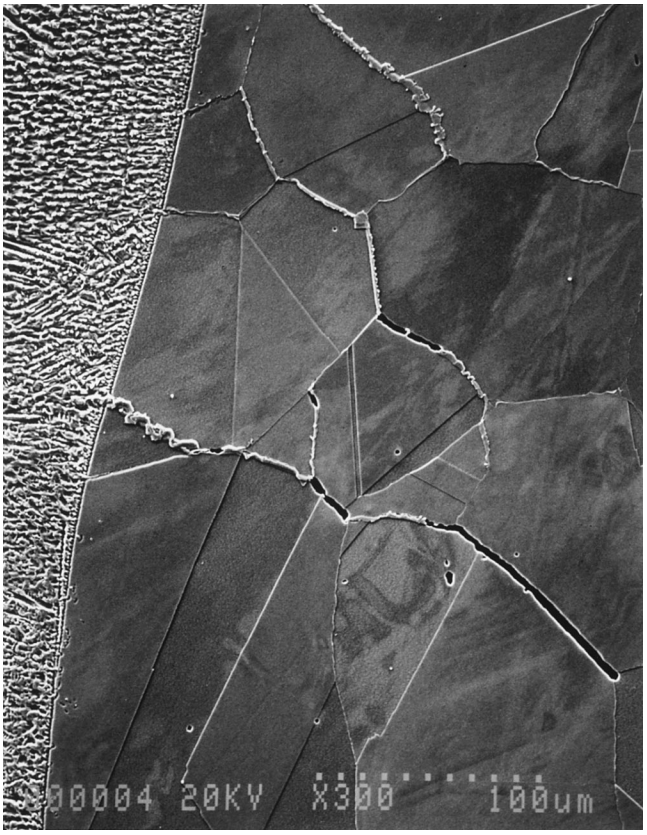

(*a*)

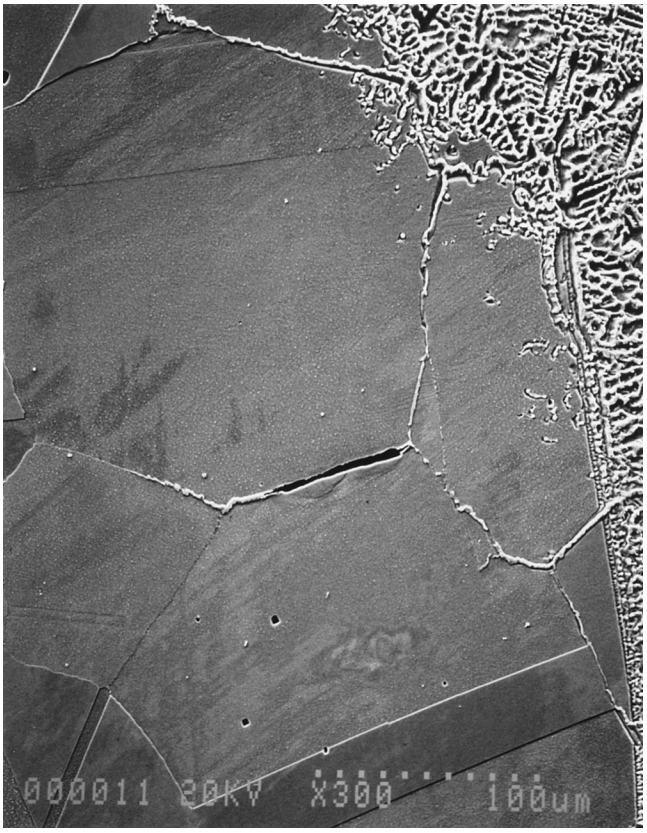

(*b*)

Fig. 10—Comparison of microfissures in HAZ in (*a*) high boron alloy and (*b*) low boron alloy.

Fig. 11—SEM image showing microfissures in HAZ of high boron alloy subjected to the solution treatment at 1150 °C for 5.5 min and followed by air cooling.

amount of Nb in the surrounding area reaches about 10 wt pct (or less, depending on the cooling rate), as suggested by the solidification constitution phase diagram for INCONEL 718.[38] As heating continues, the melting of the Nb-rich matrix spreads to a larger area, and the liquid penetrates along grain boundaries. When cooling starts, tensile stresses build up around the liquid and microfissures open in liquated boundaries, and, at the same time, resolidification of γ and Laves phases takes place along liquid microcracks at grain boundaries. Therefore, one of the characteristic features in the formation of microcracks due to constitutional liquation is the presence of resolidified products around them.

The previous features, at times, appear to be at variance with the observations of the present investigation. Although microcracks were seen at grain boundaries that had experienced melting, many of them were also associated with those that did not exhibit strong evidence of melting (Figure 11). In addition, often microcracks were not observed in the HAZ next to the fusion zone, but rather in a region slightly remote from it. It is suggested that this inconsistency is the combined result of the melting and solidification temperature of the grain-boundary material and of thermal stresses present at the grain boundaries, which appear to be quite different from the microcracking caused by constitutional liquation of Nb carbides.

The melting temperature of the boron-segregated grain boundary depends on the concentration of boron at the first few monolayers of atoms. It has been found that the boron segregation was as high as 36.7 at. pct in a 50-nm-wide zone around the grain-boundary surface in a 316L stainless

steel that contained 40 ppm of B and was heat treated at 1250 °C and air cooled at 13 °C/s.[15,16] According to the Ni-B phase diagram,[39] this monolayer could have a melting point as low as 1018 °C. This temperature is significantly lower than the melting temperature of the grain-boundary material that experienced constitutional liquation of Nb carbides, which is about 1200 °C or higher, depending on the Nb concentration in the surrounding matrix.[38] This comparison suggests that boron-segregated grain boundaries could start to melt at a temperature nearly 200 °C lower on heating during welding and would remain liquated to a temperature which is 200 °C lower than that for liquation-associated cracking caused by constitutional liquation. As heating continues, atoms next to the first few monolayers on the grain-boundary surface may also start to melt, resulting in wider melted grain boundaries, as observed in Figure 8. For the grain boundary with minor segregation of boron, the eutectic melting starts at about 1095 °C, according to B-Ni phase diagram.[39]

During the cooling cycle of welding, the solidification of melted grain boundaries will take place. The final reaction involving Laves phases should be completed at the eutectic reaction temperature, which is about 1200 °C.[38] In contrast, the solidification temperature of grain boundaries melted as a result of boron segregation can be as low as 1095 °C, which is nearly 100 °C lower than that in the case of constitutional liquation. This suggests that the melting and resolidification of boron-segregated grain boundaries occurs over a much wider temperature range than that of grain boundaries containing Nb carbides. This makes the segregation of B much more detrimental in causing HAZ liquation cracking than liquation of NbC.

It should be noted that liquation cracking occurs by the opening of liquated grain boundaries. In the case of constitutional liquation of Nb carbides, thermal stresses with a tensile nature should exist at the eutectic reaction temperature (1200 °C). In contrast, the resolidification of boron-segregated grain boundaries occurs around 1095 °C. Analysis of stresses during welding has shown that the residual stresses in the HAZ are more tensile when the temperature is high, but become compressive as the weldment is cooled to a lower temperature.[40] This suggests that the thermal stresses might have changed from tensile in nature to compressive when melted grain boundaries caused by boron segregation started to solidify. The compressive stresses prohibit the opening-up of grain boundaries and, therefore, the formation of microcracks. This might be the reason why liquation cracks were also observed at times not associated with those grain boundaries that exhibited a wide degree of liquation. However, it is also possible that liquid migrating along the grain boundary may have healed the cracks.

In the region slightly remote from the fusion zone, grain-boundary melting was probably limited to one or a few atom layers across the grain-boundary surface. Evidence of melting and resolidification at these grain boundaries, therefore, might be beyond the resolution limit of the scanning electron microscope used. Grain-boundary solidification in this region should also start much earlier than that in the region next to fusion zone, since the temperature in the former region is lower. The thermal stress in the region close to the fusion zone, however, was likely to be tensile in nature at the beginning of cooling cycle and would also decrease with an increase in the distance from the fusion zone.[40] These tensile stresses might have been retained over the temperature range over which grain boundaries solidified. As a result, liquation cracking could have developed in a region slightly remote from the fusion zone.

IV. CONCLUSIONS

Susceptibility to HAZ cracking during electron-beam welding was studied in two INCONEL 718–based alloys doped with different levels of boron. By lowering the carbon, sulfur, and phosphorous concentrations to a level as low as possible, the HAZ cracking was related directly to the level of segregation of boron at grain boundaries, which occurred by nonequilibrium segregation during the preweld heat treatment.

1. The study has demonstrated a direct correlation between the amount of boron segregated at grain boundaries and the susceptibility to HAZ cracking, in terms of the crack length and number of cracks observed in the HAZ.
2. Melting/resolidification occurred at grain boundaries in the HAZ as a result of boron segregation. The HAZ cracks were observed along the grain boundaries that had experienced extensive melting; however, a few of them were also associated with those that liquated to a smaller extent.
3. The analysis suggests that the melting and resolidification temperatures of boron-segregated grain boundaries can be about 100 °C to 200 °C lower than those of the grain boundaries that experience constitutional liquation of Nb carbides. The lower melting point of the grain-boundary material would widen that temperature range over which the grain boundaries would remain liquated, while resolidification at a lower temperature might have coincided with the change of stresses from tensile to compressive, which may prevent the development of microcracks at the liquated grain boundaries that solidified at the lower temperature.

ACKNOWLEDGMENTS

The authors thank the consortium of Manitoba aerospace industries and Natural Sciences and Engineering Research Council of Canada for the financial support.

REFERENCES

1. D.S. Duvall and W.A. Owczarski: *Welding J.*, 1967, vol. 46, pp. 423s-432s.
2. W.A. Owczarski, D.S. Duvall, and C.P. Sullivan: *Welding J.*, 1966, vol. 45, pp. 145s-155s.
3. J.J. Pepe and W.F. Savage: *Welding J.*, 1967, vol. 46 (9), pp. 411s-422s.
4. B. Radhakrishnan and R.G. Thompson: *Metall. Trans. A*, 1993, vol. 24A, pp. 1409-22.
5. R.G. Thompson, D.E. Mayo, and B. Radhakrishnan: *Metall. Trans. A*, 1991, vol. 22A, pp. 557-67.
6. R.G. Thompson and S. Genculu: *Welding J.*, 1983, vol. 62 (12), pp. 337s-345s.
7. W.A. Baeslack and D. Nelson: *Metallography*, 1986, vol. 19, pp. 371-79.
8. N.L. Richards, X. Huang, and M.C. Chaturvedi: *Mater. Characterization*, 1992, vol. 28, pp. 179-87.
9. J.C. Borland: *Br. Welding J.*, 1961, Nov., p. 526.

10. W.F. Savage and B.M. Krantz: *Welding J.*, 1966, Jan., pp. 13s-25s.
11. D. Mclean: *Grain Boundaries in Metals*, Oxford University Press, Oxford, United Kingdom, 1957.
12. E.D. Hondros and M.P. Seah: *Int. Metall. Rev.*, 1977, Dec., pp. 262-300.
13. T.M. Williams, A.M. Stoneham, and D.R. Harries: *Met. Sci.*, 1976, vol. 10, pp. 14-19.
14. R.G. Faulkner: *J. Mater. Sci.*, 1981, vol. 16, pp. 373-83.
15. L. Karlsson, H. Norden, and H. Odelius: *Acta Metall.*, 1988, vol. 36, pp. 1-12.
16. L. Karlsson and H. Norden: *Acta Metall.*, 1988, vol. 36, pp. 13-24.
17. Xu Tingdong, Song Shenhua, Yuan Zhexi, and Yu Zongsen: *J. Mater. Sci.*, 1990, vol. 25, pp. 1739-44.
18. K.A. Taylor: *Metall. Trans. A*, 1992, vol. 23A, pp. 107-19.
19. J.H. Westbrook and K.T. Aust: *Acta Metall.*, 1963, vol. 1, pp. 1151-63.
20. X.L. He, Y.Y. Yu, and J.J. Jonas: *Acta Metall.*, 1989, vol. 37, pp. 147-61.
21. X.L. He, M. Djahazi, J.J. Jonas, and J. Jackman: *Acta Metall.*, 1991, vol. 39, pp. 2295-2308.
22. V.P. Kujanpaa, S.A. David, and C.L. White: *Welding J.*, 1987, vol. 66 (8), pp. 221s-228s.
23. J.C. Lippold: *Welding J.*, 1983, vol. 62 (1), pp. 1s-11s.
24. D.S. Duvall and W.A. Owczarski: *Welding J.*, 1996, vol. 45 (8), p. 356s.
25. R.G. Thompson, B. Radhakrishnan, and D.E. Mayo: *J. Phys.*, 1988, vol. 49 (10), p. 471.
26. B. Radhakrishnan and R.G. Thompson: *Metall. Trans. A*, 1992, vol. 23A, pp. 1783-99.
27. X. Huang, N.L. Richards, and M.C. Chaturvedi: *3rd Int. SAMPE Metals and Metals Processing Conf.*, 1992, F. Froes, W. Wallace, R. Cull, and E. Struckholt, eds., Toronto, SAMPE, Covina, CA, 1992, p. M474.
28. X. Huang, N.L. Richards, and M.C. Chaturvedi: *Metall. Mater. Trans. A*, 1996, vol. 27A, pp. 785-90.
29. M.C. Chaturvedi, W. Chen, A. Saranchuk, and N.L. Richards: *Superalloys 718, 625, 706 and Various Derivatives*, E.A. Loria, ed., The Minerals, Metals, & Materials Society, 1997, pp. 743-52.
30. T.J. Kelly: in *Advances in Welding Science and Technology*, S.A. David, ed., ASM INTERNATIONAL, Metals Park, OH, 1986, pp. 623-27.
31. W. Chen, M.C. Chaturvedi, N.L. Richards, and G. McMahon: *Metall. Mater. Trans. A*, 1998, vol. 29A, pp. 1947-54.
32. P.E. Busby, M.E. Warga, and C. Wells: *Trans. TMS-AIME*, 1953, vol. 197, pp. 1463-68.
33. A. Oradei-Basile and J.F. Radavich: in *Superalloy 718, 625 and Various Derivatives*, E.A. Loria, ed., TMS, Warrendale, PA, 1991, pp. 325-55.
34. Xu Tingdong and Song Shenghua: *Acta Metall.*, 1989, vol. 37, pp. 2499-2506.
35. Hugh Baker: *ASM Handbook*, vol. 3, *Alloy Phase Diagrams*, The Materials Information Society, 1992, p. 2.304.
36. H. Guo, N.L. Richards, and M.C. Chaturvedi: *Sci. Technol. Welding Joining*, 1998, vol. 3 (5), pp. 257-59.
37. R.G. Thompson, J.J. Cassimus, D.E. Mayo, and J.R. Dobbs: *Welding J.*, 1985, vol. 64 (4), pp. 91s-96s.
38. G.A. Knorovsky, M.J. Cieslak, T.J. Headley, A.D. Romig, Jr., and W.F. Hammetter: *Metall. Trans. A*, 1989, vol. 20A, pp. 2149-58.
39. K.E. Spear: *Applications of Phase Diagrams in Metallurgy and Ceramics*, NBS Special Publication 496, NBS, Washington, D.C., 1978, vol. 2, pp. 744-62.
40. K. Masubuchi: in *Modeling of Casting and Welding Processes*, H.D. Brody and D. Apelian, eds., TMS-AIME, 1981, p. 223.